Deterioration mode of barium-containing NO_x storage catalyst

Bo-Hyuk Jang, Tae-Hun Yeon, Hyun-Sik Han [a], Yong-Ki Park [b] and Jae-Eui Yie *

Ajou University, School of Chemical Engineering, San 5, Wonchon, Suwon, Kyungki, Korea
[a] Heesung Engelhard Co., R&D Center, 16B-12, 455, Moknae, Ansan, Kyungki, Korea
[b] Korea Research Institute of Chemical Technology, Yusong, Taejon 305-600, Korea

Received 20 April 2001; accepted 15 August 2001

Barium-containing NO_x storage catalyst showed serious deactivation under thermal exposure at high temperatures. To elucidate the thermal deterioration of the NO_x storage catalyst, four types of model catalyst, Pt/Al_2O_3, Ba/Al_2O_3, $Pt–Ba/Al_2O_3$, and a physical mixture of $Pt/Al_2O_3 + Ba/Al_2O_3$ were prepared and their physicochemical properties such as BET, NO TPD, TGA/DSC, XRD, and XPS were evaluated while the thermal aging temperature was increased from 550 to 1050 °C. The fresh $Pt–Ba/Al_2O_3$ showed a sorption capacity of 3.35 wt%/g-cat. but the aged one revealed a reduced capacity of 2.28 wt%/g-cat. corresponding to 68% of the fresh one. It was found that this reduced sorption capacity was directly related to the deterioration of the NO_x storage catalyst by thermal aging. The Ba on Ba/Al_2O_3 and $Pt–Ba/Al_2O_3$ catalysts began to interact with alumina to form Ba–Al solid alloy above 600 °C and then transformed into stable $BaAl_2O_4$ having a spinel structure. However, no phase transition was observed in the Pt/Al_2O_3 catalyst having no barium component, even after aging at 1050 °C.

KEY WORDS: NO_x storage catalyst; deactivation mode; $Pt–Ba/Al_2O_3$; $BaAl_2O_4$

1. Introduction

As automobile emission regulations become strict, it is more and more important to control automotive exhaust levels. For engines that operate in a stoichiometric air/fuel condition, as do most of today's gasoline vehicles, toxic exhausts such as carbon monoxide and nitrogen oxides can be transformed successfully into the safe compounds carbon dioxide, water and nitrogen by use of a three-way catalyst (TWC). However, efforts to increase the air : fuel ratio in order to improve fuel efficiency have a negative effect on the TWC, due to the surplus of oxygen [1]. When the TWC is exposed to an excess oxygen environment, the reduction activity of NO_x decreases rapidly. In order to compensate for this reduced catalytic activity, the TWC has been enhanced by introducing NO_x storage components [2–7]. This modified TWC system known as the "NO_x storage catalyst" has been regarded as a plausible alternative for the abatement of NO_x exhausted in lean-burning gasoline engines.

Usually, the NO_x storage catalysts are composed of three main components of a high surface area substrate, noble metals and a NO_x adsorbent and are used with a type of monolith honeycomb wash-coated with these catalytic components. More specifically, γ-alumina, Pt–Rh alloy and BaO are used as the substrate, noble metals and NO_x adsorbent, respectively [3]. This $Pt–Rh–Ba/Al_2O_3$ catalyst has two main functions of NO_x adsorption and reduction, which is applied in a gasoline engine that operates alternatively under lean and rich conditions. During these repeated lean–rich cycles, the exhausted NO_x is adsorbed by the BaO adsorbent and then reduced by the Pt–Rh catalyst. Summarizing the previous results [2,8], the following scheme could be suggested for the reduction of NO_x by this NO_x storage catalyst: (i) during the lean condition, NO is oxidized to NO_2 by the noble metals and then stored into the NO_x adsorbent; (ii) then, the adsorbed NO_2 reacts with oxygen or metal carbonate to form metal nitrate; (iii) during the rich condition, the nitrate decomposes into NO_2 and metal oxide; (iv) finally, the released NO_2 is reduced to N_2 by CO or hydrocarbon over noble metal and the metal oxide reacts with CO_2 to form metal carbonate.

As suggested in the above reaction scheme, the NO_x storage component plays an important role while completing the whole reduction cycle of NO_x, and its sorption capacity should be maintained to guarantee the catalytic activity of the NO_x storage catalyst. According to the result of Fekete *et al*. [9], when barium-containing NO_x storage catalyst was exposed to temperatures above 800 °C, serious deactivation was observed due to the loss of NO_x storage capacity. However, the details of the deterioration of this NO_x storage catalyst, $Pt–Ba/Al_2O_3$ by the thermal aging have not been provided, yet. In this study, we tried to elucidate the deterioration mode of the NO_x storage catalyst, focusing on the change in NO_x storage capacity.

2. Experimental

2.1. Preparation of catalysts

To investigate the thermal deactivation process of barium-containing NO_x storage catalyst, four different types of supported catalysts were prepared by impregnating a precious metal (Pt/Al_2O_3), a NO_x storage component (Ba/

* To whom correspondence should be addressed.

1011-372X/01/1100-0021$19.50/0

Table 1
Specifications of the prepared catalysts.

Catalyst	Pt/Ba loading (wt%)	BET area (m^2/g)	Remarks
Pt/Al_2O_3	5/0	144	Fresh catalyst
Pt/Al_2O_3 (850 °C)	5/0	126	Aged at 850 °C for 24 h
Ba/Al_2O_3	0/15	115	Fresh catalyst
Ba/Al_2O_3 (850 °C)	0/15	112	Aged at 850 °C for 24 h
$Pt–Ba/Al_2O_3$	5/15	109	Fresh catalyst
$Pt–Ba/Al_2O_3$ (850 °C)	5/15	107	Aged at 850 °C for 24 h
$Pt–Ba/Al_2O_3$ (950 °C)	5/15	94	Aged at 950 °C for 24 h
$Pt–Ba/Al_2O_3$ (1050 °C)	5/15	80	Aged at 1050 °C for 24 h
$Pt/Al_2O_3 + Ba/Al_2O_3$	5/0 + 0/15	132	Physical mixture

Al_2O_3) and both of them ($Pt–Ba/Al_2O_3$) on an alumina support, and by physically mixing Pt/Al_2O_3 and Ba/Al_2O_3, as shown in table 1. Specifically 5 wt% of Pt and 15 wt% of Ba were impregnated on the γ-alumina (HIQ®-7214F, Alcoa Industrial Chemical Co.) using aqueous solutions of platinum ($H_2Pt(OH)_6$, Heesung Engelhard Corp.) and barium acetate ($Ba(OAc)_2$, Noah Technologies Corp.). The preparation procedures may be described briefly as follows: The γ-alumina powder was wetted incipiently with the aqueous solutions containing platinum or barium and then dried at 120 °C for 2 h and calcined at 550 °C for 4 h in an air atmosphere; for the preparation of the $Pt–Ba/Al_2O_3$ catalyst containing both Pt and Ba, platinum was impregnated procedurally on the Ba/Al_2O_3 catalyst; for thermal aging, the fresh catalysts were exposed further at 800, 950 and 1050 °C for 24 h in an air-circulated muffle furnace.

2.2. Characterization

The deterioration mode of the NO_x storage catalyst was monitored by several physicochemical methods, such as BET surface area, NO_x TPD, TGA/DSC (thermal gravimetric analyzer/differential scanning calorimeter), XRD (X-ray diffraction), and XPS (X-ray photoelectron spectroscopy).

2.2.1. BET surface area

The specific surface areas of the fresh and aged catalysts were determined by the BET method after nitrogen adsorption in a micropore analyzer (Micromeritics, 2200A). Before N_2 adsorption, all of the catalysts were evacuated at 250 °C for 3 h.

2.2.2. NO_x TPD and TGA

The mass and heat changes during the thermal annealing of catalysts, as well as the adsorption/desorption characteristic of NO_x were monitored using TGA/DSC (Netzsch Co., model STA 409 EP) while raising the temperature by 10 °C/min from 20 to 900 °C under different gas flows – 100 ml/min air flow for the TGA and 40 ml/min 2000 ppm NO/air flow for the NO_x TPD, respectively.

2.2.3. XRD

The XRD spectra were obtained using an automatic 2θ diffractometer equipped with a Cu Kα X-ray source (1.5406 Å, Mac Science Co.). The cluster sizes of platinum and barium were determined by the following equation [10]:

$$t\ (\mathrm{nm}) = \frac{k\lambda}{\beta \cos\theta_B},$$

where k is the correction coefficient (1.5921), λ the wave length of the X-ray source (1.5406 Å for Cu K_α), β the FWHM of the XRD peak (°), and θ_B is θ at peak maximum (°).

2.2.4. XPS

The binding energies of the catalytic compositions were measured by an X-ray photoelectron spectrometer equipped with a Mg Kα X-ray source and hemispherical sector analyzer (ESCA Lab Mk II, VG Scientific Co.). During the analysis, chemical shifts of 3–5 eV depending on the samples were observed, due to the charging effect, and they were corrected based on the contamination peak (carbon or hydrocarbon) at 284.6 eV.

3. Results and discussion

3.1. Deactivation mode of the NO_x storage catalyst

As reported by Fekete *et al.* [9], when the NO_x storage catalyst was aged under hydrothermal conditions at 750 °C for 24 h, the conversion efficiency of NO_x dropped significantly from 86 to 55% at 450 °C due to the decreased NO_x adsorption capacity, even though the optimum temperature region for adsorption/reduction of NO_x remained unchanged (figure 1(a)). Another interesting point is that contrary to the decreased NO_x adsorption capacity, a 10% improvement in hydrocarbon conversion efficiency was observed in the aged NO_x storage catalyst (figure 1(b)). This result means that the deterioration of the aged NO_x storage catalyst is caused mainly by the decreased NO_x storage capacity of the adsorbent, rather than by the reduced reduction activity of the three-way catalyst.

Following the explanation of Fekete *et al.*, the reduced adsorption efficiency could be attributed to two different deactivation modes. One is the formation of mixed metal oxides such as aluminates, zirconates, and titanates through the reaction of adsorbents and washcoat ingredients (alumina, zirconia, or titania). The other is a substantial loss of interface between precious metal and adsorbent leading to the reduced spill-over rate of NO_2 from the precious metal to the adsorbent due to the significant particle growth of both. These two explanations are both plausible, but in this study it was found that the former is the more decisive cause of the decreased NO_x reduction activity in an aged NO_x storage catalyst, and more detailed physicochemical investigations were carried out to provide clear evidence for the deterioration of the NO_x storage catalyst.

3.2. NO_x sorption capacity

For the NO_x storage catalyst to be effective, NO_x species have to be stored well in the catalyst during the lean period

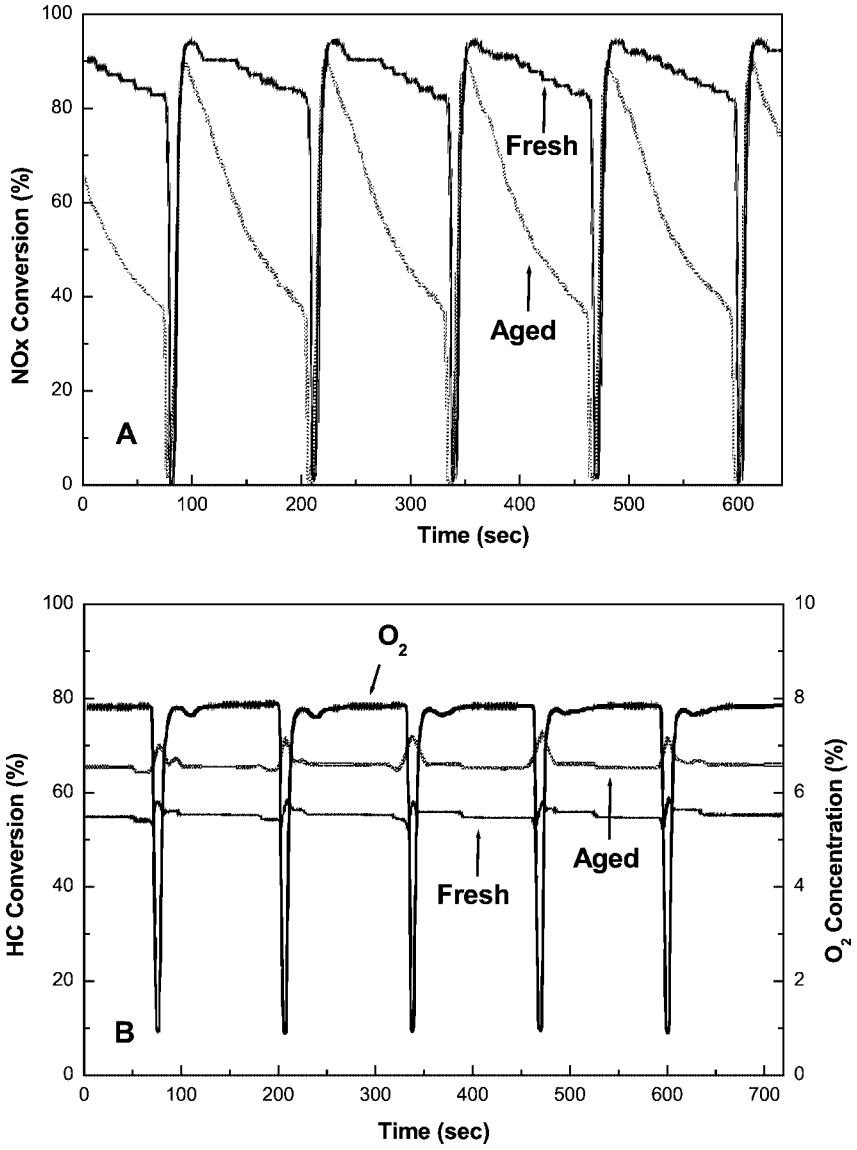

Figure 1. (A) NO_x conversion efficiency and (B) hydrocarbon conversion efficiency during the lean (120 s)–rich (6 s) cycle test for fresh (full line) and furnace aged (dotted line) Pt–Ba/Al_2O_3, LNC 6 catalysts at 450 °C (gas composition: rich = 4 vol% CO + 1.3 vol% H_2 + 444 vppm C_3H_8 + 889 vppm C_3H_6 + 750 vppm NO + 10 vol% CO_2 + 10 vol% H_2O in N_2 balance; lean = 8.0 vol% O_2 + 444 vppm C_3H_8 + 889 vppm C_3H_6 + 750 vppm NO + 10 vol% CO_2 + 10 vol% H_2O in N_2 balance; details of the preparations are described in [9]).

of operation, and these stored NO_x species have to be released and subsequently reduced during the rich condition. Therefore, the sorption capacity of NO_x is an important parameter for deciding the performance of a NO_x storage catalyst. To measure the sorption and release characteristics of NO_x, temperature-programmed adsorption and desorption cycles were repeated continuously three times on the fresh and aged Pt–Ba/Al_2O_3 catalysts and physical mixture of Pt/Al_2O_3 and Ba/Al_2O_3 while sweeping the temperature up and down from RT to 600 °C in the flowing condition of 2000 ppm NO_x/air (figure 2). Among the three adsorption/desorption cycles, the first cycle was carried out differently from the next two cycles to discriminate physisorbed and chemisorbed NO_x species. That is, in the first cycle, prior to the desorption, the catalysts were exposed in NO_x flowing at room temperature, enough for physical and chemical saturation, while in the next two cycles the desorption was carried out only after exposing the catalysts at a minimum of 200 °C, for chemisorption without physisorption. Therefore, during the first desorption cycle, both physisorbed and chemisorbed NO_x species were observed, but in the next two desorption cycles only chemisorbed NO_x species were observed, which are effective for NO_x storage in the lean phase of engine operation. Along with the fresh and aged Pt–Ba/Al_2O_3 catalysts, the sorption capacity of physically mixed Pt/Al_2O_3 + BaO/Al_2O_3 was also measured to check the extent of Pt–BaO interfacing leading to the spill-over of NO_2 from the Pt to the BaO during lean operation. Interestingly, all of the fresh, aged and physically mixed catalysts showed quite different behaviors for the first and the next two desorption cycles. In the first desorption cycle, fresh and physical mixture catalysts

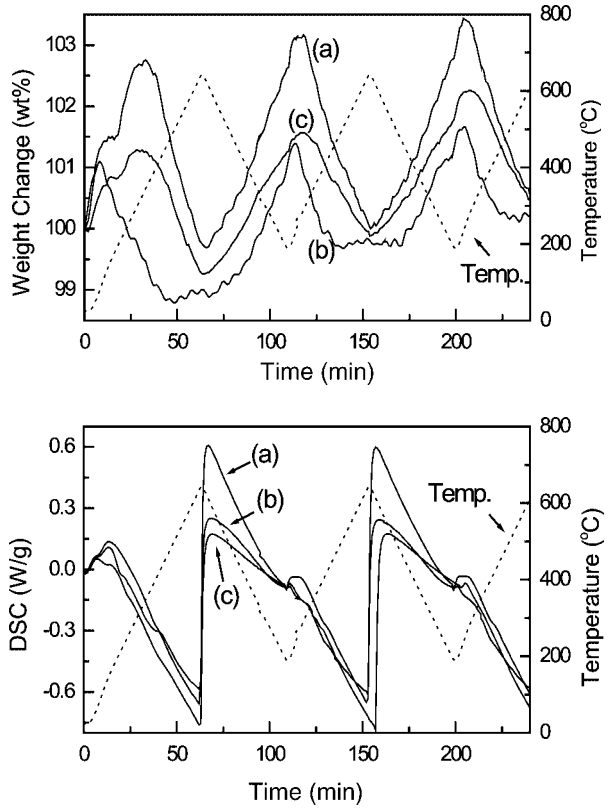

Figure 2. Three temperature-programmed adsorption/desorption cycles in 2000 ppm NO/air flowing over (a) fresh Pt–Ba/Al_2O_3, (b) Pt–Ba/Al_2O_3 aged thermally at 850 °C for 24 h, and (c) physically-mixed Pt/Al_2O_3 + Ba/Al_2O_3.

showed two desorption peaks at 120 and 330 °C, corresponding to the physisorbed and chemisorbed NO_x species, but the aged catalyst showed only one main desorption peak at 120 °C with reduced peak intensity at 330 °C. This means that the reduced sorption capacity of the thermally aged catalyst is mainly due to the decreased sorption site of NO_x at high temperatures. According to the result of Fridell *et al.* [3], in a NO_x storage catalyst containing three-way components (Pt–Rh/Al_2O_3 catalyst) and a NO_x storage component (BaO/Al_2O_3 catalyst), all of the NO_x storage capacity is attributed to the NO_x storage component, BaO/Al_2O_3. This suggests that the reduced sorption capacity of NO_x in a thermally-aged Pt–Ba/Al_2O_3 catalyst is caused mainly by the change in chemical state of BaO on alumina.

As Fekete *et al.* suggested [9], there are two main factors affecting the sorption capacity of the NO_x storage catalyst. One is the loss of sorption capacity by the change in chemical state of BaO and the other is the poor interface between Pt and BaO leading to the loss of NO_2 spillover. Comparing the sorption capacity of fresh Pt–Ba/Al_2O_3 and physically mixed Pt/Al_2O_3 + BaO/Al_2O_3, no differences were observed in adsorption and desorption behaviors except decreased sorption capacity (figure 2 and table 2). That is, the physically mixed Pt/Al_2O_3 + BaO/Al_2O_3 catalyst showed 70% of the sorption capacity of the fresh Pt–Ba/Al_2O_3 catalyst at the same adsorption and desorption temperatures. These adsorption and desorption behaviors reveal that the

Table 2
Sorption capacity of NO_x storage catalysts.

Catalyst	NO_x sorption capacity[a]
Fresh Pt–Ba/Al_2O_3	3.35 wt%/g-cat.
Aged Pt–Ba/Al_2O_3	2.28 wt%/g-cat.
Physical mixture of Pt/Al_2O_3 + Ba/Al_2O_3	2.03 wt%/g-cat.

[a] Averaged NO_x sorption capacity of 2nd and 3rd cycles.

chemical states of fresh BaO on Pt–Ba/Al_2O_3 and physically mixed Pt/Al_2O_3 + BaO/Al_2O_3 catalysts are the same but the spill-over rate of NO_2 from the Pt metal sites into the BaO adsorbents is lower in the physically mixed catalyst than in the homogeneously mixed Pt–Ba/Al_2O_3 due to the lack of interface between Pt and BaO. Contrary to the physically mixed Pt/Al_2O_3 + BaO/Al_2O_3 catalysts, however, the thermally aged Pt–Ba/Al_2O_3 catalyst has a quite different reason for its reduced sorption capacity. That is, the thermally-aged and the physically-mixed catalysts showed a similar reduced sorption capacity of NO_x, 70% that of the fresh catalyst, but the desorption temperature of NO_x was much lower in the thermally-aged catalyst than in the physically-mixed one. The lower temperature shift could be attributed to the change in chemical state of BaO.

Therefore, a systematic physicochemical analysis including TGA/DSC, XRD, ESCA, and BET was carried out to monitor the chemical state of BaO in Pt–Ba/Al_2O_3 during the thermal aging.

3.3. TGA analysis

Four different types of fresh and thermally-aged catalysts were prepared, having combinative catalytic compositions of Al_2O_3, Pt/Al_2O_3, Ba/Al_2O_3, and Pt–Ba/Al_2O_3, respectively, and TGA/DSC analyses were carried out while heating the catalysts from RT to 900 °C by 10 °C/min in flowing air (figure 3). The fresh and the aged catalysts showed different temperature dependencies in the TG analysis. In the case of fresh catalysts (figure 3A), the TGA spectra could be divided into two types, depending on the compositions of the catalysts. The barium-containing catalysts such as Ba/Al_2O_3 and Pt–Ba/Al_2O_3 showed a deflection in TGA spectra from 620 to 720 °C while no deflections were seen in the catalysts containing no barium species (figure 3A (a) and (b) *vs.* (c) and (d)). This means that the thermal treatment of the catalysts at over 600 °C in the presence of barium brings about some changes in the catalyst phase through the interaction of barium and alumina. The interaction temperature was also influenced by the presence of the Pt. The Pt–Ba/Al_2O_3 catalyst showed a deflection in mass from 620 °C, while the Ba/Al_2O_3 containing no Pt showed a deflection from 670 °C (figure 3A (c) and (d)). Through the presence of Pt, the interaction temperature of barium and alumina was lowered 50 °C. However, we do not know exactly why the interaction temperature was lowered by the Pt. More detailed experiments are needed for the determination of the cause.

Once the barium-containing catalyst was aged thermally above 850 °C, it transformed into more stable phases and no

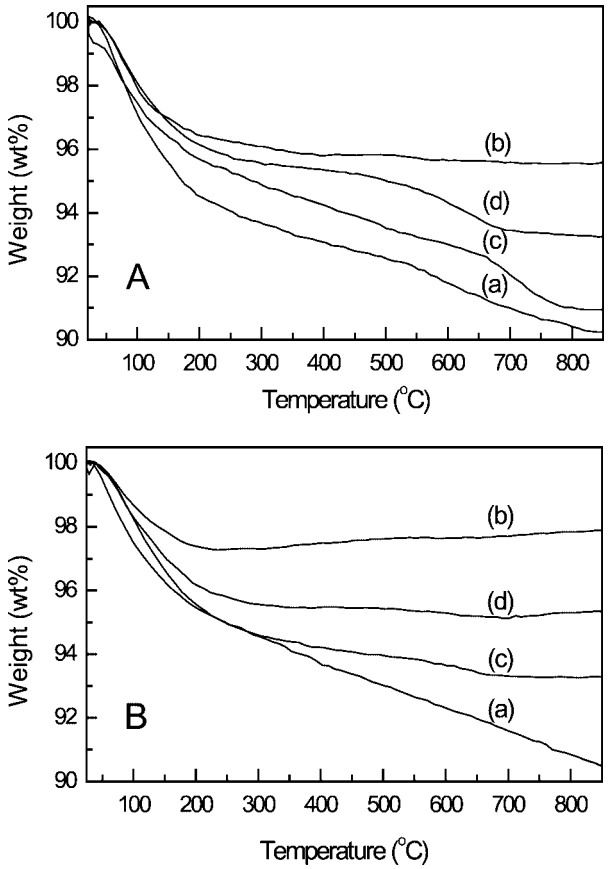

Figure 3. TGA spectra of fresh (A) and thermally-aged at 850 °C for 24 h (B) catalysts in 40 ml/min flowing air and 10 K/min heating rate: (a) Al_2O_3, (b) Pt/Al_2O_3, (c) Ba/Al_2O_3, and (d) $Pt–Ba/Al_2O_3$.

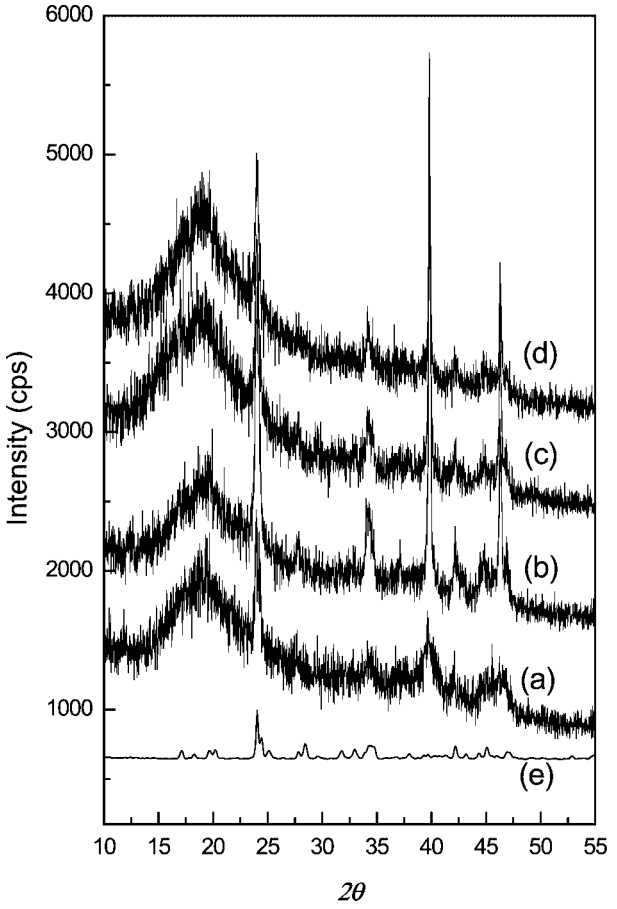

Figure 4. XRD spectra of Pt/Al_2O_3 catalysts treated for 24 h at (a) 550 °C, (b) 850 °C, (c) 950 °C, (d) 1050 °C, and (e) $BaAl_2O_4$ powder.

more changes in mass occurred during the TG analysis. That is, none of the thermally-aged catalysts, regardless of composition, showed any deflection in TGA spectra (figure 3B). Though it is not possible to discriminate what species are formed, these TGA results provide good evidence for the formation of new species through the interaction of barium and alumina during thermal aging.

3.4. Determination of Ba structure by X-ray diffraction

As observed in the TGA analysis, BaO on alumina support began to interact with alumina from around 640 °C leading to the formation of a new solid phase, with heat generation as well. Therefore, to monitor the change of structure more carefully, XRD analysis was carried out for the two types of catalysts, Pt/Al_2O_3 and $Pt–Ba/Al_2O_3$ while treating the catalysts at different temperatures, and compared with that of $BaAl_2O_4$.

As shown in figure 4, the Pt on alumina, Pt/Al_2O_3, revealed four types of strong characteristic peaks at 2θ value of 19°–20°, 23°–25°, 39°–41°, and 46°–47° corresponding to the (111), (200), (311), and (400) phases of Pt [11]. On the fresh Pt/Al_2O_3 treated at 550 °C, two main phases of (111) and (200) at 19°–20° and 23°–25° were observed with small ones at 39°–41° and 46°–47°. However, as the thermal aging temperature increased from 550 to 850 °C the peak intensities of the (311) and (400) phases at 39°–41° and 46°–47° increased, and maintained constant level without further increase of intensities above 850 °C (figure 4 (c), (d) and (e)).

In the case of $Pt–Ba/Al_2O_3$ containing both Pt and BaO, several types of new XRD peaks at 2θ value of 19.6°, 28.3°, 34.3°, and 42°–43°, distinguished from those of Pt/Al_2O_3, were observed (expressed with asterisk marks (*) in figure 5) even though the main peaks at 23°–25° could not be used to monitor the phase transition of barium during the thermal aging, due to the overlap with that of Pt(200). The fresh $Pt–Ba/Al_2O_3$ treated at 550 °C for 4 h revealed only XRD peaks originating from Pt the same as those observed on the Pt/Al_2O_3 and the intensities of other peaks were too low to be detectable. As the aging temperature increased from 550 to 850 °C, the new peaks at 19.6°, 28.3°, 34.3°, and 42°–43° began to appear and their intensities increased gradually as the aging temperature increased further. These new peaks were assigned to (222), (242), and (424) phases of $BaAl_2O_4$ based on the reference [11c]. This result is quite different from that of the Pt/Al_2O_3 where all the peaks were fully developed above 850 °C. This means that the Pt on alumina forms stable crystalline clusters having (111), (200), (311), and (400) phases above 850 °C and maintains its structure up to 1050 °C, but the Ba on alumina is not as stable as Pt and gradually transforms into a solid mixture of Ba and

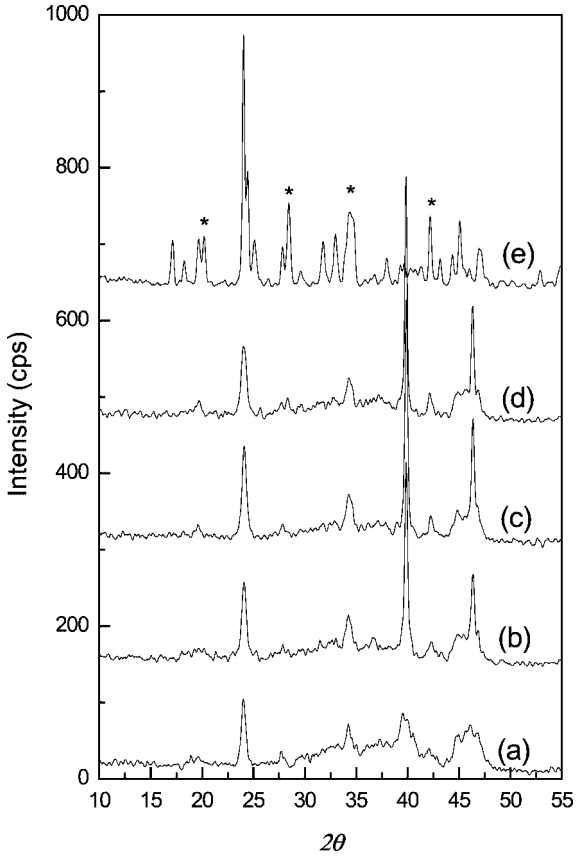

Figure 5. XRD spectra of Pt–Ba/Al_2O_3 catalysts treated for 24 h at (a) 550 °C, (b) 850 °C, (c) 950 °C, (d) 1050 °C, and (e) $BaAl_2O_4$ powder.

Al having the structure of $BaAl_2O_4$. Through the interaction of Ba and Al, several types of solid mixtures expressed as $Ba_xAl_yO_{(2x+3y)/2}$ could be formed but as found in figure 5(e) and reference [11c], the $BaAl_2O_4$ having a spinel structure of $M^{II}M^{III}_2O_4$ was formed during the thermal aging above 850 °C. That is, the new XRD peaks formed on the aged Pt–Ba/Al_2O_3 could be assigned successfully as those of $BaAl_2O_4$ even though the main peaks at 23°–25° overlapped with that of Pt/Al_2O_3. Fekete *et al.* also suggested that the main reason for the deactivation of an aged NO_x storage catalyst containing BaO, TiO_2, ZrO_2, and Al_2O_3 ingredients is the formation of mixed oxide alloys such as $BaAl_2O_4$, $BaZrO_3$, and $BaTiO_2$ [9]. However, they observed only $BaZrO_3$ and $BaTiO_2$ phases through XRD studies and failed to observe the formation of $BaAl_2O_4$. This could be explained by the slow formation rate of $BaAl_2O_4$ at low temperatures. They aged their NO_x storage catalyst at only 750 °C for 24 h but this temperature and time were not enough to make the $BaAl_2O_4$ phase fully developed. As illustrated in figure 5, even after thermal treatment at 850 °C for 24 h, the $BaAl_2O_4$ phase was not fully developed and a more severe aging condition, at least 1050 °C for 24 h, was required. This means that although the original state of BaO on Al_2O_3 could not be preserved above 750 °C, it takes quite a long time for this BaO to transform into a stable $BaAl_2O_4$ phase through the interaction of BaO and Al_2O_3. Summarizing the results of XRD and NO_x adsorption/desorption cycles, it may be deduced that even though the Pt–Ba/Al_2O_3 revealed reduced sorption capacity of NO_x after aging at 850 °C for 24 h, as shown in adsorption/desorption cycles of NO_x (figure 2), the stable $BaAl_2O_4$ phase was not fully developed in this aging condition. That is, once the Pt–Ba/Al_2O_3 catalyst is exposed thermally above 850 °C, mixed solid alloys, not even structurally definable as $BaAl_2O_4$, are formed through the interaction of BaO and Al_2O_3, and these reduce the sorption capacity of NO_x, which eventually are changed irreversibly into a stable phase of $BaAl_2O_4$.

Table 3
Particle sizes[a] of Pt and BaO on Pt–Ba/Al_2O_3 catalyst depending on the thermal aging temperature.

Temperature (°C)	$2\theta_B$		β		Particle size (nm)	
					Pt	Ba
550	39.70	34.22	1.42	0.42	1.84	7.06
850	38.22	34.24	0.21	0.61	12.42	4.86
950	39.80	34.26	0.22	0.69	11.86	4.30
1050	39.80	34.28	0.15	0.69	17.39	4.30

[a] Determined by the equation described in [10].

Table 4
Binding energy[a] of Ba($3d_5$), O(1s), Pt(4f), C(1s), and Al(2p) for fresh and aged Pt/Al_2O_3 and Pt–Ba/Al_2O_3 catalysts.

Element	Pt/Al_2O_3		Pt–Ba/Al_2O_3	
	Fresh	Aged	Fresh	Aged
Ba($3d_5$)	–	–	779.9	780.1
O(1s)	531.3	531.1	531.1	531.1
Pt(4f)	315.9	314.7	315.2	315.0
C(1s)	284.7	284.7	284.6	284.7
Al(2p)	70.7, 74.4	74.4	74.2	74.2

[a] Binding energies are corrected based on the contamination peak (carbon or hydrocarbon).

To see the effect of thermal aging on the interface between the Pt catalyst and NO_x storage component BaO, the particle size of Pt and BaO was monitored while treating the catalysts at different temperatures (table 3). On the fresh Pt–Ba/Al_2O_3 catalyst, the Pt existed in a homogeneously dispersed state having a particle size of 1.84 nm. When treated at 850 °C, its size increased rapidly to 12.4 nm and maintained a constant level during further increases up to 1050 °C. As the aging temperature increased further, the size of the Pt grew to 17.4 nm. This means that the Pt on alumina is stable in a certain temperature range of 550–1050 °C, but it is not stable above 1050 °C and agglomerates into big clusters. The opposite trend was observed for the Ba on alumina. The Ba on fresh Pt–Ba/Al_2O_3 revealed a particle size of 7.06 nm and its size decreased to 4.3 nm as the aging temperature increased to 1050 °C. According to the result of Hodjati *et al.* [12], the sorption capacities of the NO_x storage catalyst are more strongly influenced by the phase of sorption components than by the existence of Pt. Our result also revealed that the Pt on alumina was quite stable in the aging temperature window and the sorption capacities of NO_x were affected more severely by the transformation of the Ba phase on alumina than by the sintering of Pt.

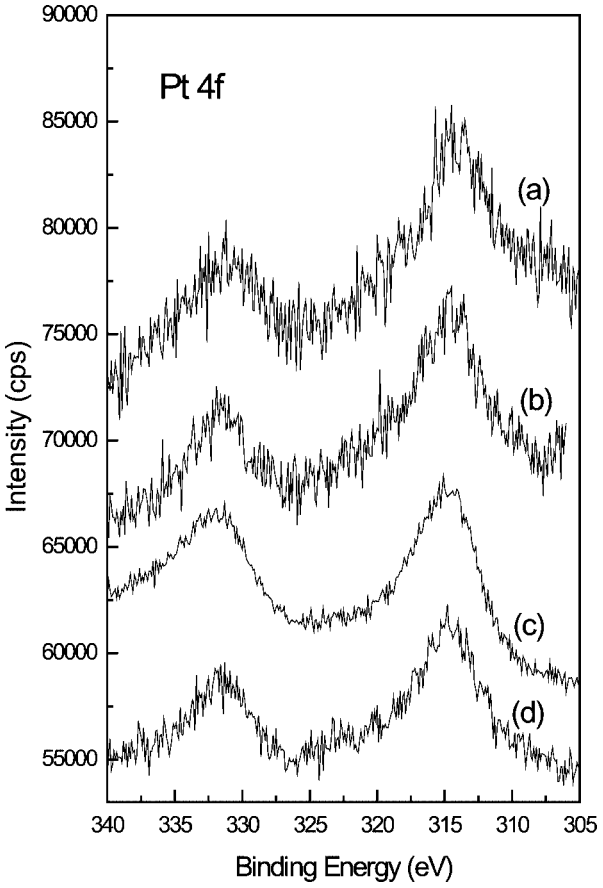

Figure 6. XPS spectra of Pt(4f): (a) fresh Pt/Al_2O_3, (b) Pt/Al_2O_3 aged at 850 °C, (c) fresh $Pt–Ba/Al_2O_3$, and (d) $Pt–Ba/Al_2O_3$ aged at 850 °C.

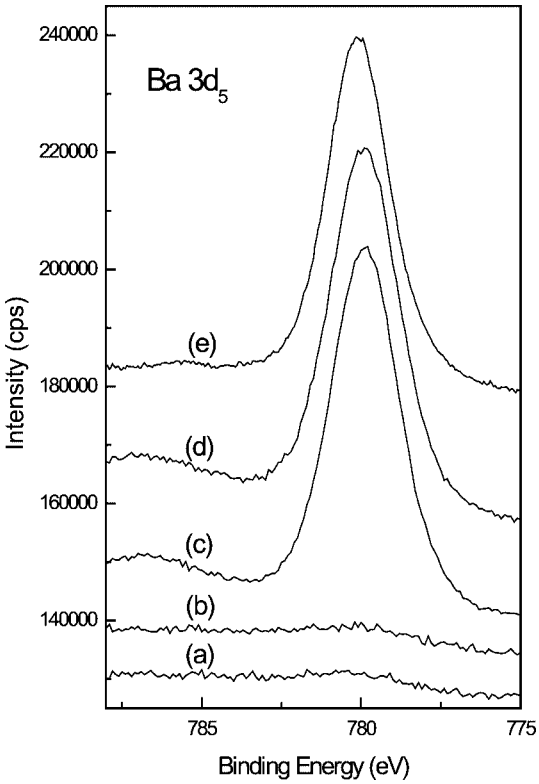

Figure 7. XPS spectra of $Ba(3d_5)$: (a) fresh Pt/Al_2O_3, (b) Pt/Al_2O_3 aged at 850 °C, (c) fresh $Pt–Ba/Al_2O_3$, (d) $Pt–Ba/Al_2O_3$ aged at 850 °C, and (e) $BaAl_2O_4$.

3.5. Chemical analysis by XPS

The chemical state of catalytic components such as Pt, Al, and Ba were monitored by X-ray photoelectron spectroscopy while changing the aging temperature and catalytic compositions (figures 6–8 and table 3). As shown in figures 6 and 7, among the three catalytic components, the Pt and Ba showed a constant value of binding energies regardless of types of catalysts and whole treatment conditions. That is, their binding energy changes were too small to permit interpretation of the chemical state of the catalysts during the thermal aging process.

However, different from the Pt and Ba, the binding energy of Al showed a trend dependent on the thermal aging conditions (figure 8). In the case of Pt/Al_2O_3 containing no Ba component, the binding energy of Al was constant for all of the fresh and aged catalysts (figure 8 (a) and (b)). That is, the same binding energy of 74.4 eV corresponding to the Al(2p) of alumina was obtained with the fresh and aged catalysts [13]. However, the fresh $Pt–Ba/Al_2O_3$ containing both Ba and Al showed a new Al(2p) peak at a lower binding energy of 70.7 eV, corresponding to the chemical shift of −3.5 eV, along with the peak at 74.4 eV (figure 8(c)). This lower chemical shift is thought to be caused by the BaO dispersed on the alumina support due to the difference in electronegativity. When the aluminum and barium exist together,

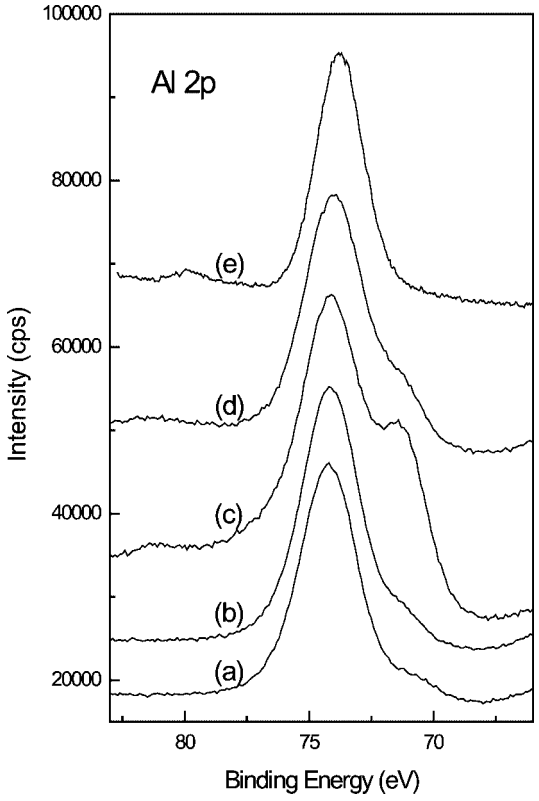

Figure 8. XPS spectra of Al(2p): (a) fresh Pt/Al_2O_3, (b) Pt/Al_2O_3 aged at 850 °C, (c) fresh $Pt–Ba/Al_2O_3$, (d) $Pt–Ba/Al_2O_3$ aged at 850 °C, and (e) $BaAl_2O_4$.

the electron is transferred from the less electronegative barium to the more electronegative aluminum, which resulted in the lower shift of binding energy for aluminum. When the Pt–Ba/Al_2O_3 was aged at 850 °C for 24 h, the intensity of this peak decreased and appeared as a small shoulder on the main peak at 74.4 eV. In terms of binding energy, due to having the same binding energy as that of alumina, it seemed that this new phase returned to the alumina again but it could be interpreted differently with the help of XRD and TGA results (figures 3 and 5). According to the XRD and TGA analyses, after thermal aging a new solid phase like $BaAl_2O_4$ was formed, which revealed the same binding energy as that of alumina (figure 8(e)). Therefore, this peak could be assigned as an Al(2p) of $BaAl_2O_4$ instead of alumina. Summarizing the XPS results, there exist two different types of Al on the Pt–Ba/Al_2O_3 according to the thermal aging conditions. In the fresh state, there exists alumina isolated from BaO, but after aging at 850 °C it interacts with BaO and converts into a homogeneous solid mixture of $BaAl_2O_4$. This XPS result could also be used to estimate the state of Ba on the alumina support. In the fresh Pt–Ba/Al_2O_3, the Ba exists as an isolated BaO dispersed homogeneously on the alumina but after thermal exposure above 750 °C it converts gradually to a solid mixture of $BaAl_2O_4$ having no NO_x sorption capacity.

4. Conclusion

From the physicochemical study of the NO_x storage reduction catalyst, Pt–Ba/Al_2O_3, it was found that the reduced sorption capacity was directly related with deterioration of the NO_x storage catalyst by thermal aging, and that its reduction was caused by the phase transition of barium oxide impregnated on the alumina into the Ba–Al solid alloy eventually to the stable $BaAl_2O_4$ having a spinel structure. In all of the barium-containing catalysts, Ba/Al_2O_3 and Pt–Ba/Al_2O_3, the Ba began to interact with alumina to form a Ba–Al solid alloy at above 600 °C and then transformed into a stable $BaAl_2O_4$ at above 950 °C. Once the Ba–Al solid alloy was formed, its sorption capacity decreased to 68% of that of the fresh NO_x storage catalyst. However, no phase transition was observed in the TWC Pt/Al_2O_3 containing no barium component, even aged at 1050 °C.

Acknowledgement

This work was supported in part by Ajou University under the Research Facilities Support Program in the year 2000.

References

[1] M.S. Brogan, A.D. Clark and R.J. Brisley, SAE 980933 (1998).
[2] N. Takahashi, H. Shinjoh, T. Iijima, T. Suzuki, K. Yamazaki, N. Miyoshi, S.-i. Matsumoto, T. Tanizawa, T. Tanaka, S.-s. Tateishi and K. Kasahara, Catal. Today 27 (1996) 63.
[3] E. Fridell, M. Skoglundh, B. Westerberg, S. Johansson and G. Smeller, J. Catal. 183 (1999) 196.
[4] T. Kobayashi, T. Yamada and K. Kayano, SAE 970745 (1997).
[5] W. Bogner, M. Kramer, B. Krutzsch, S. Pischinger, D. Voigtlander, G. Wenninger, F. Wirbeleit, M.S. Brogan, R.J. Brisley and D.E. Webster, Appl. Catal. B 7 (1995) 153.
[6] S. Balcon, C. Potvin, L. Salin, J.F. Tempere and G. Djéga-Mariadassou, Catal. Lett. 60 (1999) 39.
[7] T. Nakatsuji and R. Yasukwa, SAE 980932 (1998).
[8] H. Mahzoul, J.F. Brilhac and P. Gilot, Appl. Catal. B 20 (1999) 47.
[9] N. Fekete, R. Kemmler, D. Voigtlander, B. Krutzsch, E. Zimmer, G. Wenninger, W. Strehlau, J.A.A. van den Tillaart, J. Leyrer, E.S. Lox and W. Muller, SAE 970746 (1997).
[10] J.M. Thomas and W.J. Thomas, *Principles and Practice of Heterogeneous Catalysis* (VCH, Weinheim, 1997) p. 151.
[11] (a) T. Swanson, Natl. Bur. Stand. Circ. 539 (1953) 31;
(b) L. Liu, J. Appl. Phys. 42 (1971) 3702;
(c) S.-Y. Huang, R. von der Muehll, J. Ravez and M. Couzi, Ferroelectrics 159 (1994) 127.
[12] S. Hodjati, P. Bernhardt, C. Petit, V. Pitchon and A. Kiennemann, Appl. Catal. B 19 (1998) 209, 221.
[13] C.D. Wagner, W.M. Riggs, L.E. Davis and J.F. Moulder, *A Reference Book of Standard Data: For Use in X-ray Photoelectron Spectroscopy* (Perkin–Elmer, Eden Prairie, MN).